

Brief communication: A ~50 Mm³ ice-rock avalanche on 22 March 2021 in the Sedongpu valley, southeastern Tibetan Plateau

Chuanxi Zhao^{1,2}, Wei Yang^{1,3*}, Matthew Westoby⁴, Baosheng An^{1,5}, Guangjian Wu^{1,3,6}, Weicai Wang^{1,3}, Zhongyan Wang¹, Yongjie Wang^{1,6}, Stuart Dunning⁷

5 ¹ Key Laboratory of Tibetan Environment Changes and Land Surface Processes, Institute of Tibetan Plateau Research, Chinese Academy of Sciences, Beijing, China Beijing 100101, China

² College of Earth and Environmental Sciences, Lanzhou University, Lanzhou 730000, China

³ CAS Center for Excellence in Tibetan Plateau Earth Sciences, Beijing 100101, China

⁴ Department of Geography and Environmental Sciences, Northumbria University, Newcastle upon Tyne, NE1 8ST, UK

10 ⁵ School of Science, Tibet University, Lhasa 850011, China

⁶ South-East Tibetan Plateau station for integrated observation and research of alpine environment, Lulang, China

⁷ School of Geography, Politics and Sociology, Newcastle University, Newcastle upon Tyne, NE1 7RU, UK.

Correspondence to: Wei Yang (yangww@itpcas.ac.cn)

Abstract. On 22 March 2021, a ~50 M m³ ice-rock avalanche occurred from 6500 m asl in the Sedongpu basin, southeastern Tibet. The avalanche transformed into a highly mobile mass flow which temporarily blocked the Yarlung Tsangpo river. The avalanche flow lasted ~5 minutes and produced substantial geomorphological reworking. This event, and previous ones from the basin, occurred concurrently with, or shortly after, positive seasonal air temperature anomalies. The occurrence of future large mass flows from the basin cannot be ruled out, and their impacts must be carefully considered given implications for sustainable hydropower and associated socioeconomic development in the region.

20 1 Introduction

Catastrophic mass flows originating from the mountain cryosphere can cause hazard and risk cascades that result in widespread loss of life, destruction of property, and significant geomorphological reworking (Haeberli et al., 2004; Jacquemart et al., 2020; Kääh et al., 2021; Shugar et al., 2021). Exploring the evolution of such events is important for constraining likely triggering and conditioning factors and the nature of the mass flow process chain (e.g. for improving numerical models). In
25 turn, this information can be useful for assessing the potential hazards to life and downstream assets (Evans et al., 2021; Kääh et al., 2021).

Cryospheric hazards occur frequently in the monsoon-influenced Himalayas, including the southeastern Tibetan Plateau (Kääh et al., 2021; Zheng et al., 2021), a region which hosts temperate glaciers that are typically more sensitive to changes in air temperature than continental glaciers on the Plateau interior (Wang et al., 2019). The region has undergone accelerated
30 mass loss and areal reduction of glacier extent in the past two decades (Bolch et al., 2019) and the rate of regional atmospheric warming is above the global average (Yao et al., 2019). The southeastern Tibetan Plateau contains high topographic relief conducive for the development of hazard cascades, and the region has experienced a series of high-magnitude ice-rock

35 avalanches, glacier detachments, and glacial lake outburst floods in recent decades (Tong et al., 2019; Veh et al., 2020; Kääb et al., 2021; Zheng et al., 2021). Furthermore, the region is the focus of considerable investment by [the Chinese government](#), including the construction of the high-speed Sichuan-Tibet Railway (anticipated completion 2030) [and the development of adjacent areas along this emerging economic corridor, which links the cities of Lhasa and Chengdu \(Fig. 1a\) and passes through mostly mountainous terrain. A key aspect of regional economic development includes](#) the construction of new large-scale hydropower projects to serve an increasing regional and international demand for electricity. [Mass flow hazards](#) of cryospheric origin are of significant concern across High Mountain Asia, particularly when [these flows have the potential to affect regions that are experiencing](#) rapid changes in both [the exposure and vulnerability of populations and infrastructure](#) (Shugar et al., 40 2021).

The Sedongpu basin (29.80° N, 94.92° E) in Nyingchi prefecture, [China](#), has a history of large avalanches and low-angle glacier detachments which have transformed into powerful debris flows (Tong et al., 2019; Chen et al., 2020; Wang et al., 2020; Kääb et al., 2021). The basin has a total area of 67 km² and ranges from a maximum elevation of 7294 m asl at Gyala 45 Peri peak to a minimum of ~2750 m at [the](#) confluence with the Yarlung Tsangpo, a major tributary of the Brahmaputra River (Fig. 1b). The Randolph Glacier Inventory (V6.0) identifies 18 glaciers covering a total of ~17 km² in the basin (RGI Consortium, 2017), which are nourished by snow, ice, and debris from very steep mountain flanks. Analysis of historic satellite imagery has revealed evidence of mass flow activity in the basin (Kääb et al., 2021) and at least 11 mass flows originating in the basin have partially or entirely blocked the Yarlung Tsangpo in past decade (Tong et al., 2019; Chen et al., 2020). The 50 basin recently experienced [several](#) large ice-rock avalanches ([Table S1](#)) with [an initial volume](#) of ~50 Mm³ (October 2017 and into 2018) and the detachment of the tongue of Sedongpu Glacier in two separate events with a total of ~130 Mm³ on 17/18 October and 29 October 2018 (Kääb et al., 2021). Both detachments in 2018 transformed into debris flows; the earlier detachment blocked the Yarlung Tsangpo for ~60 hours, and the rapid rise in upstream water level damaged [and](#) threatened roads, power lines, hydropower stations, and other riverside infrastructure and prompted relocation of more than 6,000 local 55 residents (Chen et al., 2020). [After the 2018 detachments, the U-shaped glacier bottom was exposed with loose debris and limited ice residue \(An et al., 2021\).](#)

In this brief communication we [document a](#) large ice-rock avalanche that [occurred outside the regular summer ablation season](#) in the Sedongpu basin on 22 March 2021 [and](#) which, similar to past events, also temporarily blocked the Yarlung Tsangpo. We [use in-situ](#) field investigations, high-resolution satellite imageries, digital elevation models, seismic records, and 60 meteorological data to analyse the evolution of the event and its impact, discuss potential drivers, and briefly [discuss](#) implications for the sustainable development of the region.

2. Data and Methods

The basin's recent event history led to the installation of time-lapse optical [and](#) thermal cameras and an automatic weather station (AWS) at the exit of the basin in September-October 2019. [Data from this station were captured and](#) transmitted [via](#)

65 [the Inmarsat maritime satellite system at a 3 hour interval](#). These instruments were installed by the [Institute of Tibetan Plateau Research, Chinese Academy of Sciences](#), for the purpose of obtaining photographic and meteorological evidence of future mass flows and their timing. A Campbell CS477 radar-based water level monitoring system [has been installed](#) at Gyala, which is located on the Yarlung Tsangpo ~6 km upstream of the exit of the Sedongpu basin (Fig. 1b), [and provides a real-time \(10 min interval\) record of water level](#). [In addition to generating data of scientific value, the system was used for local alerting of rising water level caused by the temporary damming of the Yarlung Tsangpo](#). We used a DJI Phantom 4 [unpiloted aerial vehicle](#) to obtain aerial photographs of the basin in October 2019 (i.e. pre-event) and on 25 March 2021 (post-event), and document [the geomorphological modification of the landscape around the basin outlet \(Fig. 1c-e and Fig. S1\)](#).

70 Vertical seismic waveforms (10 Hz) from long-period seismographs recorded at Nyingchi station, ~60 km from the Sedongpu basin, were used to determine the start time of the March 2021 event and [analyse](#) its evolution. In addition, we used United States Geological Survey (USGS) seismic and meteorological records from monitoring stations at Nyingchi, Bomi (~80 km distance) and Milin (~80 km distance) to analyse the regional tectonic and climatic context of the event.

75 We used pre- and post-event 0.5 m-resolution tri-stereo optical Pléiades images (Pléiades-1A, [captured 30 December 2018](#) and Pléiades-1B, [captured 30 April 2021](#), respectively) to [determine](#) the source location of the avalanche and [to construct](#) high-resolution (1 m) DEMs to [estimate](#) the volume and size distribution of the initial detachment and quantify net elevation change along the flow path. The DEMs were [generated photogrammetrically in PCI Geomatica software \(Banff sp4\) with the OrthoEngine module](#). A sufficient number of [ground control points](#) and [tie points](#) were also automatically collected to improve the computed math model in [the OrthoEngine module, which uses the Semi-Global Matching \(SGM\) algorithm for pixels-matching](#). And the implementation of SGM is done by image-matching along epipolar lines. We used the *demcoreg* Python package to refine horizontal and vertical alignment of the DEM data (Shean et al., 2020); the final products had a relative vertical accuracy of 0.51 ± 4.1 m over stable ground (Fig. S2).

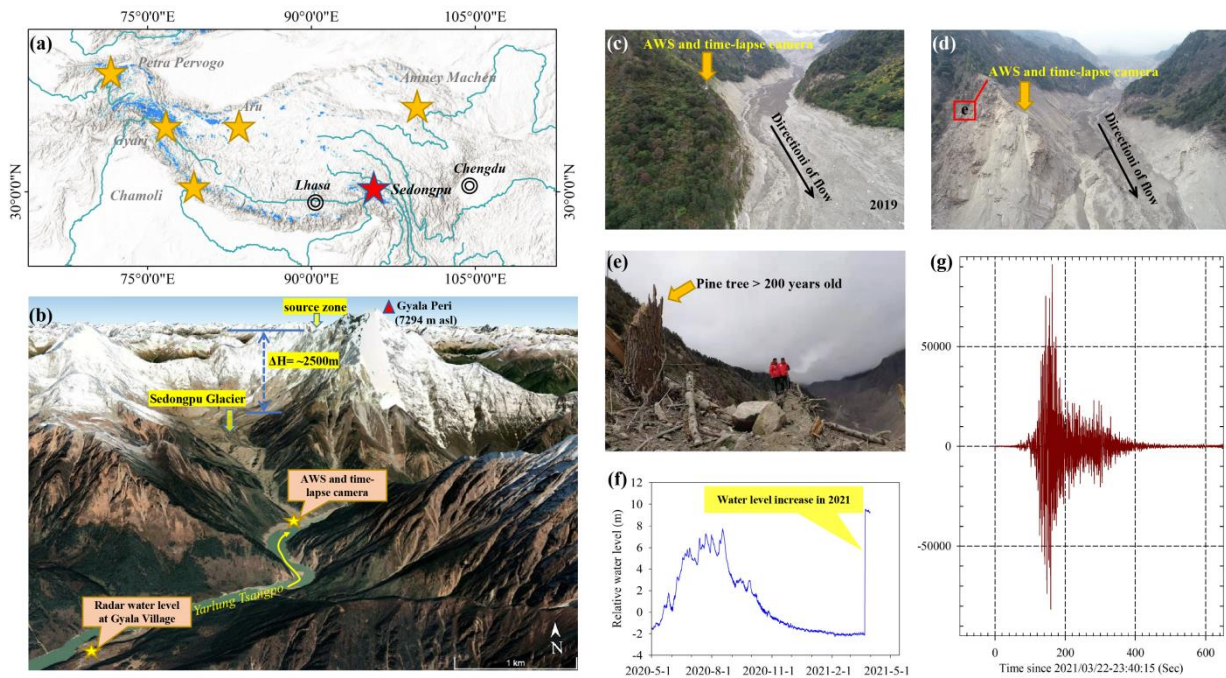


Figure 1. Overview of the Sedongpu basin, landscape modification, river blockage and seismic waveform caused by the March 2021 ice-rock avalanche. (a) Location of the Sedongpu basin and the recent reported massive glacier detachments and ice-rock avalanches in High Mountain Asia. (b) © Google Earth image (images on 2017-12-14, @CNES/Airbus and Maxar Technologies) showing topographic condition of the Sedongpu basin, the location of hazard cascade area and the ground-based observations (yellow stars). (c, d) Photographs showing the same view in October 2019 (pre-event) and on 25 March 2021 (post-event) looking into the Sedongpu valley. The photos show the location of an AWS and time-lapse camera ~150 m above the valley floor close to the valley outlet (see panel b) which were destroyed by the March 2021 event. (e) Photograph showing a mass flow-overtopped hill where the monitoring station was installed. (f) the sudden water level rise caused by the Yarlung Tsangpo river blockage on 22 March 2021. (g)– Seismic waveform recorded at the Nyingchi station, 60 km away from Sedongpu basin starting 23:40:15 March 22 2021.

3. Results and Discussion

3.1 Field observations of the March 2021 avalanche and river blockage

The last automatic data transfer from our monitoring system at the outlet of Sedongpu valley (Fig. 1b) occurred at 21:30 PM on 22 March 2021, whereafter the data feed became inactive. Shortly thereafter, our water level sensor at Gyala village sent an automatic water level warning due to a sudden 2.2 m increase in river stage between 23:50 PM on 22 March and 00:00 AM on 23 March (Fig. 1f). The water level continued to increase at a rate of 0.6 – 0.8 m/hour and rose by a total of 11 m before

105 stabilising at around 18:00 PM on 23 March (Fig. S3). Both data streams (or sudden lack thereof) implied the blockage of the
Yarlung Tsangpo, likely by a large mass flow event, and, along with seismic data (Fig. 1g), were useful for constraining its
timing.

We undertook a field visit to area on 25 March 2021 and found evidence that a mass flow from Sedongpu basin had
overtopped a 200 m-high spur at the basin outlet, destroying the combined AWS-time lapse camera monitoring station and
stripping the surrounding slope of vegetation (Fig. 1d-e). This included 200 year-old pine forest, thereby indicating that no
110 event of comparable magnitude has occurred here in the past two centuries. By applying a simple frictionless point mass model
of $u = \sqrt{2hg}$ (Iverson et al., 2016) where h is runup height (~200 m), calculated by differencing handheld GPS locations on
the valley bottom and the highest elevation destroyed trees, and g is the gravitational constant, we estimate that a flow velocity
(u) of around 60 m s^{-1} (~225 km/h) is required for overtopping the 200 m-high valley spur. Post-event field observations
showed the valley bottom to be covered by fresh, water-rich debris which was in the process of dewatering, and widespread
115 destabilisation of valley flanks along the flow path (Fig. 1d and Fig. S1).

Examination of the seismic record at Nyingchi station reveals the onset of a clear ground-shaking event at 23:41 PM on 22
March (Fig. 1g). The seismic waveform has the typical characteristics of a landslide because it lacks the clear P- and S-wave
arrival times typical for earthquakes (Ekström and Stark, 2013). The waveform suggests that the avalanche-mass flow lasted
~300 seconds and consisted of an initial phase (lasting 100 s) exhibiting a high-amplitude signal which we infer as representing
120 the detachment and downslope passage of the initial ice-rock avalanche, followed by a ~200-second waveform with a weaker
amplitude, which most likely reflects the passage of the continuous mobile mass flow through the Sedongpu basin and its
outlet valley. Based on the duration of the seismic waveform and known distances (~11 km), we estimate that the mean velocity
of the whole avalanche-mass flow possibly reached $\sim 37 \text{ m s}^{-1}$ (~132 km/h). These observations and inferences were
corroborated by local people at Gyala village, who report hearing a continuous, ‘loud’ sound originating from the direction of
125 the Sedongpu basin at this time (pers. comm.).

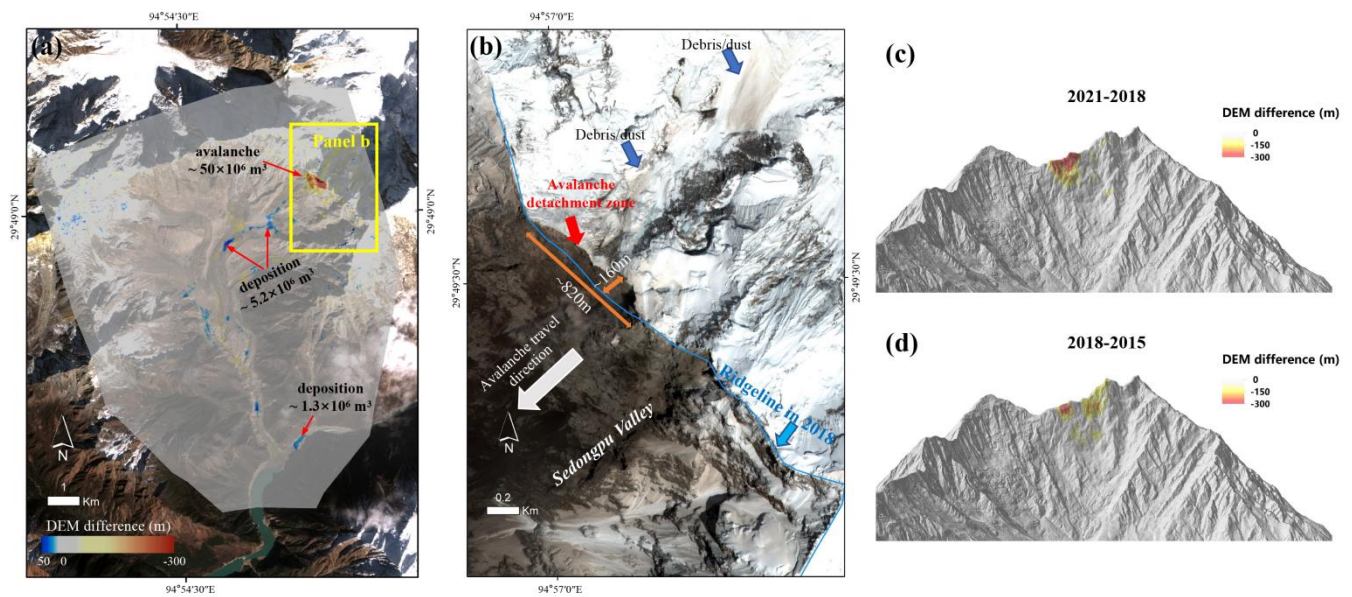


Figure 2. Elevation change across the wider Sedongpu basin derived from Pléiades imagery dated 30 December 2018 and 30 April 2021 (a). The zoomed Pléiades image on 30 April 2021 showing the headward migration of the mountain ridgeline due to mass loss associated with the March 2021 ice-rock avalanche (b). Oblique three-dimensional comparison of source regions and magnitudes of the massive ice-rock avalanches in 2021 and 2017 near the north ridge of Gyala Peri peak (c,d).

3.2 Avalanche source, magnitude and landscape change

The comparison of 0.5 m-resolution Pléiades satellite orthophotos (dated 30 December 2018 and 30 April 2021) and field investigation revealed that the avalanche originated from the western flank of a ridge that extends north from Gyala Peri (Fig. 2a). DEM differencing reveals that about $\sim 50.0 \pm 1.5 \text{ Mm}^3$ of ice and rock detached from the mountain ridge (Fig. 2c). We assume that the majority of this material was released in the March 2021 event as we have not detected any large avalanching events capable of transforming into a debris flow since the October 2018 glacier detachment. The mean and maximum depth of surface lowering in the source detachment area was $\sim 140 \text{ m}$ and $\sim 300 \text{ m}$, respectively, and the detachment scar spans an altitudinal range of $\sim 6000 - 6500 \text{ m asl}$, across a horizontal area of $\sim 0.36 \text{ km}^2$. The avalanche caused headward erosion of the ridgeline of up to $\sim 160 \text{ m}$, over $\sim 800 \text{ m}$ laterally (Fig. 2b).

We posit that the avalanche contained a mixture of rock and glacier ice; a perched ice mass was on the ridgeline pre-event (Fig. S4), whilst the ‘fresh’ appearance of the rock face immediately beneath the ridge implies the incorporation of at least some rock debris, but we remain uncertain on the exact ice/rock ratio. Existing analysis of past events in the basin shows the potential for a high proportion of rock debris in the initial detachment (Kääb et al., 2021). Videography by the corresponding author captured in October 2019 (see Supplementary Information) shows an avalanche originating from approximately the same source region on the mountain ridgeline as the March 2021 event. From its appearance, the avalanche appears to be

comprised mostly of ice and snow to begin with, and transitions to comprise more rock and debris later in the video, which provides some site-specific insight into how the composition of such events can transform following an initial detachment.

150 Post-event field photographs and Pléiades orthophotos show that the source area of the March 2021 ice-rock avalanche is located <0.5 km to the north of the large (17 and 33 Mm³) avalanches which occurred in 2017 (Fig. 2d and Kääb et al., 2021).

155 Whilst the vast majority of material from the March 2021 avalanche descended downslope to the west into the Sedongpu basin, a post-event Pléiades orthophoto (30 April 2020) shows evidence of small-scale ice and rock avalanching into the adjacent catchment to the east of the ridgeline (Fig. 2b). We detect 5.2 Mm³ of net deposition at the foot of the avalanche region within a slope-distance of 3.5 km from the source. A further 12.4 Mm³ was deposited along the flow path lower down in the Sedongpu valley, and at least 1.3 Mm³ was deposited in the form of a temporary dam on the Yarlung Tsangpo (Fig. 2a). We speculated that the ‘missing’- ice-rock material from the avalanche source area was either dispersed thinly along and adjacent to the flow path on the valley bottom, the neighbouring glaciers and the outlet of valley basin (Fig. S5a), or directly entered the Yarlung Tsangpo river (Fig. S5b), which was difficult to detect using DEM differences. We therefore infer that the

160 flow was highly mobile, an observation in line with previous events in the basin (Kääb et al., 2021) and elsewhere (Shugar et al., 2021). Whilst we do not focus in detail on the impacts of the avalanche and mass flow further downstream, post-event satellite imagery reveals elevated turbidity in the Brahmaputra River at Xirang, ~200 km from the avalanche source and close to the disputed international border with India, less than 36 hours after the event, demonstrating the far-reaching, international influence of large mass flows from the Sedongpu basin in a region that is geopolitically sensitive.

165

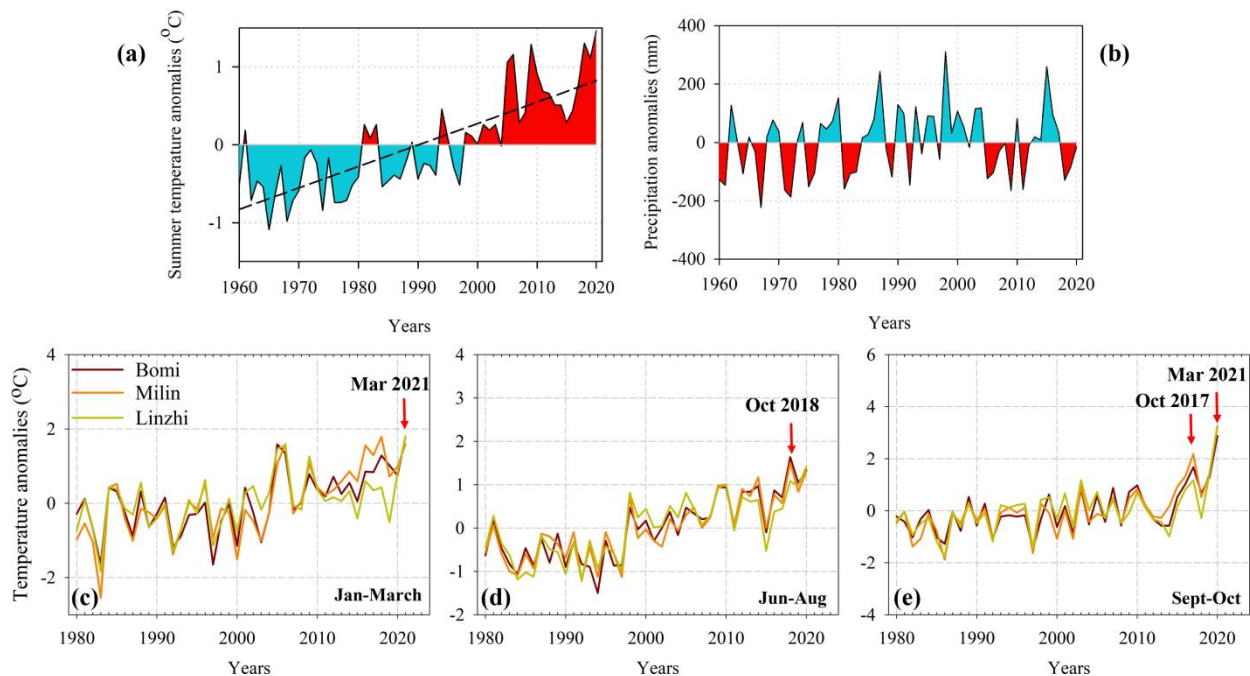


Figure 3. Anomalies of mean air temperature during the ablation season (June-September) and the total annual precipitation at the Nyingchi station, showing the significant air temperature rising (the dashed black line) at the rate of 0.28 °C/decade ($p < 0.001$) (a,b). Anomalies of minimum air temperature relative to the mean value for the period 1980-2021, recorded by the three nearest meteorological stations (Bomi, Milin, Nyingchi). The timings of the avalanche events that occurred in October 2017, October 2018 and March 2021 are shown for context (c-e).

3.3 Possible drivers for the 2021 ice-rock avalanche

The Gyala Peri region, and the southeastern Tibetan Plateau more broadly, are tectonically active. Seismic activity, a known mass movement avalanche trigger, has been proposed as a possible trigger mechanism for avalanche-driven debris flows originating from the Sedongpu valley in 2017 and into 2018 (Zhao et al., 2019). Indeed, the Gyala Peri region is seismically active and has experienced >20 earthquakes >M3.5 during the period 2000-2020, which is higher than other nearby glacierized centres (e.g. Fig. S6). Whilst we do not detect heightened seismic activity around the time of the March 2021 avalanche, it is possible that seismic activity over preceding years and decades may have been a conditioning (rather than triggering) factor. Frequent earthquakes, particularly the M6.9 earthquake on 18 November 2017 and small magnitude aftershocks near the Gyala Peri mountain (Zhao et al., 2019) may have enhanced any pre-existing cryospheric instabilities, especially in the high mountain ridges where topographic amplification can occur.

Meteorological records from nearby monitoring station show a significant increase in mean air temperature but insignificant change for annual total precipitation change (Fig. 3a-b). Similar to the so-called ‘Chamoli event’ (Shugar et al. 2021), the March 2021 Sedongpu event occurred during an exceptionally warm period outside of the ‘regular’ summer ablation season. We found that the 2021 ice-rock avalanche, and previous ones from the basin, occurred concurrently with, or shortly after the record of positive air temperature anomalies (Fig. 3c-e for mean minimum air temperature, Fig. S7 for mean air temperature). The period January to March 2021 saw positive temperature anomalies in the range +1.6 - +1.8 °C, and which exceeded (Nyingchi: 2991 m asl, Bomi: 2737 m asl) or came close to exceeding (Milin: 2950 m asl) historical records (Fig. 3e). Similarly, in 2017 and 2020 we observe unprecedented positive temperature anomalies in the months of September and October at all three stations (+2.0 - 3.3 °C); the former coincides with the occurrence of the October 2017 ice-rock avalanche in the Sedongpu basin, whilst the record positive temperature anomalies in Autumn 2020 and late Winter-early Spring 2021 occur immediately before, and during, the period when the March 2021 avalanche occurred (Fig. 3e). In addition, the summer in 2018 was the warmest season during the past four decades; the mean air temperature during June-August was 0.95-1.3 °C higher than the historical mean for this period (Fig. 3d). The extrapolated half-hourly air temperature by using the AWS records near the Sedongpu basin outlet and the constant lapse rate of -0.60 °C/100m evidenced discontinuous positive air temperature at the avalanche source region (6500 m asl) during the period from May to October. It is well-established that climatic warming can initiate complex feedback mechanisms in high-mountain regions; permafrost thaw and associated reductions in rock strength, and the warming of glacier beds, can lead to enhanced instability and the initiation of mass movements (Falaschi et al., 2019; Shugar et al., 2021).

Whilst it is difficult to directly attribute the March 2021 avalanche to atmospheric warming, it is likely that a series of factors including i) topographic disposition, ii) recent and long-term seismic activity; iii) the destabilising influence of long-term regional warming on the mountain cryosphere, and iv) recent extreme positive temperature anomalies, leading to v) increased meltwater lubrication at the bed of perched ice masses and infiltration into the bedrock fracture network may have directly or indirectly contributed to the initiation of the March 2021 ice-rock avalanche and ensuing debris flow.

4. Conclusions and Implications

Our data and accompanying analysis provide insight into the source, process, magnitude and impacts of the massive 22 March 2021 ice-rock avalanche which originated in the Sedongpu basin and temporarily dammed the Yarlung Tsangpo river. The March 2021 event, and notable events that have preceded it (e.g. ~50 Mm³ ice-rock avalanche, 2017-2018, and the ~130 Mm³ glacier detachment in October 2018), reinforce the classification of the basin as a hotspot of catastrophic mass flow activity. The basin is also located within the wider Yarlung Tsangpo ‘Grand Canyon’ which is earmarked for the development of large-scale hydropower and associated socioeconomic development in coming decades. We suggest that ongoing ground- and remote sensing-based observation of this basin, and similar basins more widely across the southeastern Tibetan Plateau, should be a priority for the research community, as should predictive modelling for exploring the influence of, for example,

sustained deglaciation, permafrost thaw, and short-lived and longer-term atmospheric warming on the stability of the mountain cryosphere in this region. Finally, we emphasise the importance of targeted engagement with relevant stakeholders to ensure that hazards of cryospheric origin are considered within the remit of sustainable development, including the reduction of risk to life and property along potential mass flow pathways.

220

Data availability. Data are available upon request from the corresponding author. We utilised PlanetScope (www.planet.com) image IDs 20210310_033352_64_245d (March 10), 20210323_033244_29_2451 (23 March) and 20210324_035901_1040 (24 March) to analyse river turbidity and identify the sediment plume from the 22 March Sedongpu event in the Brahmaputra River at Xirang. Long-period seismographs were provided by the Data Management Centre of the China National Seismic Network at the Institute of Geophysics, China Earthquake Administration and are available on request. The meteorological data for Nyingchi, Bomi and Milin stations are available from Chinese Meteorological Data Service Center (<http://data.cma.cn>). USGS earthquake data are from <https://www.usgs.gov/natural-hazards/earthquake-hazards/lists-maps-and-statistics>

225

230

Competing interests. The authors declare that they have no conflict of interest.

Author contribution. All authors conceived the study and [contribute variously to data collection](#), [processing](#), and [analysis](#). W.Y., Y.W., Z.W, B.A and G.W. carried out fieldwork, W.Y and C.Z. performed remote-sensing analyses. M.W and S.D contributed [to the analysis of results and](#) discussion. All authors contributed [to the writing and revision of](#) the paper.

235

Acknowledgements. The study is supported by the Second Tibetan Plateau Scientific Expedition and Research Program (STEP) (2019QZKK0201) and the National Natural Science Foundation of China (41961134035, [41988101](#)), Royal Society Newton Advanced Fellowship (NA170325) and National Key Research and Development Project (2019YFC1509102). We thank the National Climate Center, China Meteorological Administration for providing meteorological data and the USGS for the seismic data.

240 **References**

[An, B., Wang, W., Yang, W., Wu, G., Guo, Y., Zhu, H., Gao, Y., Bai, L., Zhang, F., and Zeng, C.: Process, mechanisms, and early warning of glacier collapse-induced river blocking disasters in the Yarlung Tsangpo Grand Canyon, southeastern Tibetan Plateau. *Sci. Total. Environ.*, 151652, <https://doi.org/10.1016/j.scitotenv.2021.151652>, 2021](#)

245

Bolch, T., Shea, J. M., Liu, S., Azam, F. M., Gao, Y., Gruber, S., Immerzeel, W. W., Kulkarni, A., Li, H., and Tahir, A. A.: Status and change of the cryosphere in the extended Hindu Kush Himalaya region, in: The Hindu Kush Himalaya Assessment, Springer, 209-255, https://doi.org/10.1007/978-3-319-92288-1_7, 2019.

- Chen, C., Zhang, L., Xiao, T., and He, J.: Barrier lake bursting and flood routing in the Yarlung Tsangpo Grand Canyon in October 2018, *J. Hydrol.*, 583, 124603, <https://doi.org/10.1016/j.jhydrol.2020.124603>, 2020.
- Ekström, G. and Stark, C. P.: Simple scaling of catastrophic landslide dynamics, *Science*, 339, 1416-1419, <https://doi.org/10.1126/science.1232887>, 2013.
- 250 Evans, S. G., Delaney, K. B., and Rana, N. M.: The occurrence and mechanism of catastrophic mass flows in the mountain cryosphere, in: *Snow and Ice-Related Hazards, Risks, and Disasters*, Elsevier, 541-596, <https://doi.org/10.1016/B978-0-12-394849-6.00016-0>, 2021.
- Falaschi, D., Kääb, A., Paul, F., Tadono, T., Rivera, J. A., and Lenzano, L. E.: Brief communication: Collapse of 4 Mm³ of ice from a cirque glacier in the Central Andes of Argentina, *The Cryosphere*, 13, 997-1004, <https://doi.org/10.5194/tc-13-997-2019>, 2019.
- 255 Haeberli, W., Huggel, C., Kääb, A., Zraggen-Oswald, S., Polkvoj, A., Galushkin, I., Zotikov, I., and Osokin, N.: The Kolka-Karmadon rock/ice slide of 20 September 2002: an extraordinary event of historical dimensions in North Ossetia, Russian Caucasus, *J. Glaciol.*, 50, 533-546, <https://doi.org/10.3189/172756504781829710>, 2004.
- 260 Iverson, R. M., George, D. L., and Logan, M.: Debris flow runup on vertical barriers and adverse slopes, *J. Geophys. Res. Earth. Surf.*, 121, 2333-2357, <https://doi.org/10.1002/2016JF003933>, 2016.
- Jacquemart, M., Loso, M., Leopold, M., Welty, E., and Tiampo, K.: What drives large-scale glacier detachments? Insights from Flat Creek glacier, St. Elias Mountains, Alaska, *Geology*, 48, 703-707, <https://doi.org/10.1130/G47211.1>, 2020.
- Kääb, A., Jacquemart, M., Gilbert, A., Leinss, S., Girod, L., Huggel, C., Falaschi, D., Ugalde, F., Petrakov, D., Chernomorets, S., Dokukin, M., Paul, F., Gascoïn, S., Berthier, E., and Kargel, J. S.: Sudden large-volume detachments of low-angle mountain glaciers – more frequent than thought?, *Cryosphere*, 15, 1751-1785, <https://doi.org/10.5194/tc-15-1751-2021>, 2021.
- 265 RGI Consortium. Randolph Glacier Inventory – A Dataset of Global Glacier Outlines: Version 6.0: Technical Report, Global Land Ice Measurements from Space, Colorado, USA. Digital Media. DOI: <https://doi.org/10.7265/N5-RGI-60>, 2017.
- 270 Shean, D. E., Bhushan, S., Montesano, P., Rounce, D. R., Arendt, A., and Osmanoglu, B.: A Systematic, Regional Assessment of High Mountain Asia Glacier Mass Balance, *Front. Earth Sci.*, 7, <https://doi.org/10.3389/feart.2019.00363>, 2020.
- Shugar, D., Jacquemart, M., Shean, D., Bhushan, S., Upadhyay, K., Sattar, A., Schwanghart, W., McBride, S., de Vries, M. V. W., and Mergili, M.: A massive rock and ice avalanche caused the 2021 disaster at Chamoli, Indian Himalaya, *Science*, 300-306, <https://doi.org/10.1126/science.abh4455>, 2021.
- 275 Tong, L. Q., Tu, J. N., Pei, L. X., Guo, Z. C., Zheng, X. W., Fan, J. H., Zhong, X., Liu, C. L., Wang, S. S., He, P., and Chen, H.: Preliminary discussion of the frequent debris flow events in Sedongpu Basin at Gyala Peri peak, Yarlung Zangbo River, *J. Eng. Geol.*, 26, 1552-1561, <https://doi.org/10.13544/j.cnki.jeg.2018-401>, 2019.
- Veh, G., Korup, O., and Walz, A.: Hazard from Himalayan glacier lake outburst floods, *Proc. Natl. Acad. Sci. U.S.A.*, 117, 907-912, <https://doi.org/10.1073/pnas.1914898117>, 2020.

- 280 Wang, R. J., Liu, S. Y., Shangguan, D. H., Radic, V., and Zhang, Y.: Spatial Heterogeneity in Glacier Mass-Balance Sensitivity across High Mountain Asia, *Water*, 11, <https://doi.org/10.3390/w11040776>, 2019.
- Wang, W., Yang, J., and Wang, Y.: Dynamic processes of 2018 Sedongpu landslide in Namcha Barwa–Gyala Peri massif revealed by broadband seismic records, *Landslides*, 17, 409-418, <https://doi.org/10.1007/s10346-019-01315-3>, 2020.
- 285 Yao, T. D., Xue, Y. K., Chen, D. L., Chen, F. H., Thompson, L., Cui, P., Koike, T., Lau, W. K. M., Lettenmaier, D., Mosbrugger, V., Zhang, R. H., Xu, B. Q., Dozier, J., Gillespie, T., Gu, Y., Kang, S. C., Piao, S. L., Sugimoto, S., Ueno, K., Wang, L., Wang, W. C., Zhang, F., Sheng, Y. W., Guo, W. D., Ailikun, Yang, X. X., Ma, Y. M., Shen, S. S. P., Su, Z. B., Chen, F., Liang, S. L., Liu, Y. M., Singh, V. P., Yang, K., Yang, D. Q., Zhao, X. Q., Qian, Y., Zhang, Y., and Li, Q.: Recent Third Pole's Rapid Warming Accompanies Cryospheric Melt and Water Cycle Intensification and Interactions between Monsoon and Environment: Multidisciplinary Approach with Observations, Modeling, and Analysis, *Bull. Am. Meteorol. Soc.*, 100, 423-444, <https://doi.org/10.1175/BAMS-D-17-0057.1>, 2019.
- 290 Zhao, B., Li, W., Wang, Y., Lu, J., and Li, X.: Landslides triggered by the Ms 6.9 Nyingchi earthquake, China (18 November 2017): analysis of the spatial distribution and occurrence factors, *Landslides*, 16, 765-776, <https://doi.org/10.1007/s10346-019-01146-2>, 2019.
- Zheng, G., Mergili, M., Emmer, A., Allen, S., Bao, A., Guo, H., and Stoffel, M.: The 2020 glacial lake outburst flood at Jinwuco, Tibet: causes, impacts, and implications for hazard and risk assessment, *Cryosphere*, 15, 3159-3180, <https://doi.org/10.5194/tc-15-3159-2021>, 2021.
- 295